Environmental and Climate Technologies
2021, vol. 25, no. 1, pp. 467–478
https://doi.org/10.2478/rtuect-2021-0034
https://content.sciendo.com

Electrical Conductivity and Water Effects in Phosphoric Acid Solutions for Doping of Membranes in Polymer Electrolyte Fuel Cells

Jürgen GIFFIN[1], Fosca CONTI[2]*, Carsten KORTE[3]

[1, 3] *Institute of Energy and Climate Research IEK-14: Electrochemical Process Engineering, Forschungszentrum Jülich GmbH, Jülich, Germany*

[2] *Department of Chemical Sciences, University of Padova, Padova, Via Marzolo 1, 35131 Padova PD, Italy*

***Abstract* – Fuel cells (FCs) are among the more efficient solutions to limit the emission of greenhouse gases. Based on the conversion of the chemical energy of a fuel (often hydrogen) and an oxidizing agent (often oxygen) into electrical energy, a typical FC produces a voltage of 0.7 V under load. The potential is highly increased by placing the cells in series to obtain a stacked cell. Among the types of FCs, the polymer electrolyte membrane FCs (PEMFCs) are developed mainly for transport applications, because of their low impact on the environment, high power density and light weight compared with other types of FCs. Phosphoric acid (H_3PO_4) doped polybenzimidazole (PBI) membranes are widely used as efficient electrolytes. The performance of a (high temperature, 130–200 °C) HT-PEMFC depends mainly on the amount of H_3PO_4 in the solid polymer membrane. The strong autoprotolysis of H_3PO_4 is responsible for the high proton conductivity also in the anhydrous state. In this study, the H_2O-H_3PO_4 system is investigated in the temperature range 60–150 °C with varying water vapour activity at constant atmospheric pressure. Main purpose is to gain more insights into the kinetics of the equilibria in the H_2O-H_3PO_4 system, which influence the fuel cell performance. Density, water content, electrical conductivity and activation energy are determined by exposing H_3PO_4 solutions for sufficiently long periods to controlled gas atmosphere in order to reach near-equilibrium conditions. The coexistence of ortho- and pyrophosphoric acid is analysed and higher condensed species are also considered. A new setup fully made in quartz is designed and developed to mix the phosphoric acid solutions in a climate chamber. The experimental results are compared to literature data to validate the developed setup and the methodology.**

***Keywords* – Acid doping; electrical conductivity; fuel cell; phosphoric acid; polymer electrolyte membranes; proton exchange membrane; vapor activity**

Nomenclature		
FC	Fuel cell	–
HT-PEM	High temperature polymer electrolyte membrane	–
PBI	Polybenzimidazole	–
a	Activity	–
m	Concentration	wt%
ρ	Density	$g \cdot cm^{-3}$

* Corresponding author.
E-mail address: fosca.conti@unipd.it

WE	Working electrode	–
RE	Reference electrode	–
τ	Thermal equilibration half-time	s
T	Temperature	°C
κ	Electrical conductivity	$S \cdot cm^{-1}$

1. INTRODUCTION

A fuel cell is essentially composed of an anode, a cathode, and the electrolyte, which allows ions to move between the two electrode sides of the cell while the electrons have to move though an external circuit, producing direct current electricity. The electrolyte classifies the type of the fuel cell and the operating conditions. In polymer electrolyte membrane fuel cells (PEMFC) the electrolyte is usually a proton conducting polymer membrane. PEMFCs have become a promising alternative power source for stationary, portable, and vehicular applications due to their unique advantages: quick start-up and load response, quit operation process, efficient energy conversion, and low exhaust emission [1]. However, cost, performance, and durability are still challenging aspects, which limit the widespread commercialization of PEMFCs [2].

In the last decade, biological aspects have been considered, so that microbial fuel cells have started to gain interests in addition to conventional chemical fuel cells. In such systems electrogenic bacteria convert organic biomass substrates to carbon dioxide, electrons and protons in the anodic chamber [3], [4]. However, the present study focuses on chemical FCs.

Membranes based on polybenzimidazole (PBI) and derivatives doped with phosphoric acid (H3PO4) have been proposed as very efficient electrolytes when operating a PEMFC at elevated temperatures, i.e. 130–200 °C (HT-PEMFC) [5]–[7]. In the present study, the electrical properties of H_3PO_4 are investigated in a wide temperature range. Key benefits of H_2SO_4, by comparison to other mineral acids, such as sulphuric acid (H_2SO_4), are excellent proton conductivity, no degradation reactions with the host polymer PBI and low volatility due to low vapor pressure even above 100 °C, i.e. at the temperatures intended for high-temperature PEMFC operations [8]–[10]. Another remarkable property of H_2SO_4 is in relation to water solubility, which decreases with increasing temperature. High operation temperatures are advantageous for running a PEMFC because the electrode kinetics are faster, the residual heat can be used for energy cogeneration and the CO tolerance is higher in comparison to working at lower temperatures. Moreover, using a non-aqueous proton conducting electrolyte like PBI/H_3PO_4 allows atmospheric operation without humidification of the feed gases and recycling of water. H_3PO_4 dehydrates at low water vapor partial pressure and rehydrates with increasing partial pressure. These changes are reflected in the composition of the acid and therefore in its proton conductivity, which is required for the good activity of the PEMFCs [11].

The extremely high proton conductivity of H_2SO_4 is mainly due to a strong autoprotolysis and a network of hydrogen bonds, which is highly polarizable and allows cooperative proton transport [12], [13]. Therefore, it is evident that changes in water content affect the conductivity. In addition to the protolysis equilibria, hydrolysis and condensation equilibria are the typical reactions in bulk H_2SO_4 (ortho-phosphoric acid), which lead to the formation of dimer, di-phosphoric acid $H_4P_2O_7$ (pyro-phosphoric acid), and higher oligomers as tri-phosphoric acid $H_5P_3O_{10}$, tetra-phosphoric acid $H_6P_4O_{13}$, penta-phosphoric acid $H_7P_5O_{16}$, etc. and aqueous species as H_2O and H_3O^+ [14]. The different polyacids, which coexist with an

increasing polymerization degree by temperature rise, ultimately lead to complex equilibria. Therefore, for certain temperature range and water content, different mixtures of polyacids can exist in either a stable or metastable state, depending on the kinetics of the equilibria. The variable fractions of ortho-phosphoric acid, polyacid species and water will influence the total proton conductivity of the electrolyte membrane.

In the temperature range of 100–200 °C, the water vapor pressure can vary over a large range, i.e. from 0.1 kPa to 101 kPa. Under these conditions, by dehydration, H_3SO_4 can form the condensates, which alter the global physical-chemical properties, particularly viscosity, strength of the acid, and solubility in water. The polycondensation equilibria of H_3SO_4 and the implications for proton conductivity are objects of the present study. The complexity of the condensation processes of the acid and the high dynamic of the hydrogen bonding network, where proton transfer is driven by hydrogen bonds breaking/formation of new bonds, are known to be the most important contributors of high proton conductivity at low water concentrations, such as those in HT-PEMFCs operating at 160–180 °C [15].

In this paper, density, water content, and electrical conductivity of H_3PO_4 aqueous solutions are presented and discussed with an emphasis on the temperature range relevant for FC applications, i.e. at 60, 90, 120, and 150 °C. The activation energy is considered in relation to the water content of the solutions. A new setup in quartz is designed and developed to mix the acid in a climate chamber and to measure impedance values under isothermal conditions.

2. Materials and Methods

2.1. Materials

Phosphoric acid (85 wt% H3PO4 with purity more than 99.9 %) was used as purchased from the supplier (Merck) without any further purification. Double distilled water was further purified with a Millipore line (0.055 $\mu S \cdot cm^{-1}$). The platinum meshes and wires used in the conductivity cell were chemically cleaned, rinsed and annealed in a gas flame to remove possible contaminants before every new filling of the cell.

2.2. Conductivity Measurement Setup

A new experimental setup was designed and developed with two main purposes:

- to measure the electrical conductivity of phosphoric acid solutions;
- to study the exchange processes with the water molecules inside the solutions and above them in vapor form.

The setup consists of four main parts, as depicted in Fig. 1(a): an electrochemical cell (1) is positioned on a pneumatic seesaw (2) and located inside a climate chamber (3). A personal computer controls the data acquisition and the pneumatic mechanism. The computer is interfaced to an impedance analyser (4). In Fig. 1(b) a photo of the setup is reported. Abbreviations and letters in Fig. 1 are explained in the following paragraphs.

The electrochemical cell was made of quartz because of its chemical stability towards H_3PO_4 so that no contamination of the acid was expected [16]. Indeed, by holding a quartz beaker filled with 85 wt% H_3PO_4 for a week at 280 °C and dry conditions (1.4 kPa water vapor pressure), no significant silica content was found in the acid solution, according to chemical analysis carried out using inductively coupled plasma optical emission spectrometry. Due to the low thermal expansion coefficient of quartz, the cell constant can be considered temperature independent and therefore constant.

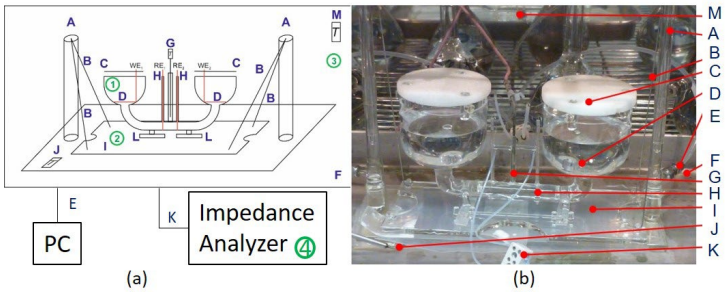

Fig. 1. In-house developed conductivity measurement setup: (a) scheme with four main parts: (1) electrochemical cell, (2) pneumatic seesaw, (3) climate chamber, (4) impedance analyser and computer controller; (b) photo of the setup showing the quartz electrochemical cell positioned on the quartz pneumatic seesaw and located inside the climate chamber.

The quartz cell is used to measure the electrical conductivity of phosphoric acid and consists of two half-cells with a diameter of 10 cm which are connected through a quartz tube having a diameter of 15 mm. The diameter of the conductivity measurement section was 15 mm, which is large enough to ensure a laminar flow during a mixing cycle due to the seesaw motion of the cell. The cell was equipped with a four-electrode arrangement made of platinum. The two reference electrodes (RE abbreviation in Fig. 1(a), i.e. electrical potential probe) consist of two platinum wires (H) while the two working electrodes (WE) consist of two coarse platinum meshes with ca. 9 cm² surface each (D). To ensure homogeneous current distribution at the potential electrodes, the working electrodes were in the reservoirs far away from the measurement site of the potential electrodes. Generally, the geometric parameters of the setup were selected in accordance with the specifications of Shreiner *et al.* [17] for electrical characterization using Jones-type conductance cells.

The measurement cell was designed to hold a maximum volume of ca. 500 ml, but electrical measurements were still possible at a reduced volume of 250 ml without influence on the electrical performance, and without refilling or decanting. To overcome the problem of concentration gradients and diffusion limited behaviour, a mechanical mixing method was implemented for the H_3PO_4 solution in the cell. Stirrers were deemed unviable due to corrosion of metal parts. Therefore, a pneumatically driven seesaw, made of quartz and operating with dry pressurized air, was designed to tilt the measurement cell. The seesaw carried the measurement cell and was steered by a customized *Festo* hardware control. Two quartz cylinders located on the left and right side of the measurement cell (A in Fig. 1) drive the pneumatic mechanism by hosting the raising/lowering components. The seesaw is hooked to the cylinders with four stainless steel rods (B in Fig. 1) since cables showed a reduced lifetime due to corrosion. Additional details in the photo of Fig. 1(b) are two glass-frit discs to cover the half-cells (C), one temperature sensor of the phosphoric acid solution (G), one plate hosting the quartz seesaw (I), one temperature sensor of the setup (J), and one temperature sensor of the climate chamber (M). Finally, E represents the connector to the hardware controller of the pneumatic mechanism via PC, while K represents the connector to the impedance analyser.

2.3. Pneumatic Mechanism and Setting Procedure

The pneumatic mechanism allows the motion of each cylinder between two positions: the powered-off position, when the cylinder is not subjected to air flow and the raised position,

when the cylinder is raised up due to the air flow mechanism. In addition, the pneumatic control mechanism allows an independent motion of the two cylinders so that the left and right cylinders can be moved separately in time sequence. A typical tilting sequence takes two minutes and has six steps per cycle from III to VIII, as indicated in Table 1. A complete mixing of liquid solution in the cell was finished at the latest after 10 min or six cycles. This mixing time was confirmed by observing the striation pattern of coloured acid solutions and by mixing coloured carboxymethyl cellulose solutions having viscosity comparable to phosphoric acid.

The cell and the seesaw were located in a 0.6 m^3 climate chamber (*Weiss WK3/600*) equipped with three *Pt100-type* temperature sensors to log and control the working temperature with an uncertainty of ±0.1 °C. The temperature sensors (sketched in Fig. 1 by three small rectangles including the letter T) were located:

1. Between the two reference electrodes of the cell (element G in Fig. 1) to detect the temperature of the H_3PO_4 solutions;
2. Under the seesaw (element J in Fig. 1) to detect the temperature of the setup;
3. In a free corner position of the climate chamber (element M in Fig. 1) to measure the temperature of the climate chamber.

The humidity was controlled below 100 °C using a psychrometric sensor and up to 160 °C using a capacitance-type humidity sensor. Both humidity sensors were factory calibrated to an accuracy of ±0.03; additional reference measurements were carried out using a dew point measurement tester (*MBW 373 HX*).

TABLE 1. STEP SEQUENCE TO TILT THE PNEUMATIC SEESAW AND THE ELECTROCHEMICAL CELL

Step	Cylinders configuration	Status	Duration, s
I	Both cylinders lowered	Maintenance position	variable
II	Both cylinders raised	Stand-by position	variable
III	Right cylinder lowering + hold	Mixing – part 1	15
IV	Right cylinder lifting + hold	Mixing – part 1	15
V	Both cylinders raised	Settling position	30
VI	Left cylinder lowering + hold	Mixing – part 2	15
VII	Left cylinder lifting + hold	Mixing – part 2	15
VIII	Both cylinders raised	Settling position	30

2.4. Experimental Measurements

In this work, the cell constant of the developed setup was measured with the four-point probe technique using two working electrodes, two potential electrodes [18] and standard KCl solutions with concentration in the range of 0.01–0.3 $mol \cdot kg^{-1}$. A cell constant of 2.02±0.01 cm^{-1} was obtained.

An *IviumStat* impedance analyser was located outside the climate chamber to measure the electrical properties of the H_3PO_4 solutions (element 4 in Fig. 1). The impedance was converted to the conductivity (κ) and each measurement was recorded after the period of time (τ), which was needed by the water content of the acid solutions to be in equilibrium with the atmosphere of the climate chamber. Therefore, the conductivity at the equilibrated condition was used as result and plotted versus water concentration (m). The error of the conductivity was found to be mostly smaller than ±0.1 %, thus indicating that sufficient data without significant scatter was acquired and the recording time was long enough.

The measurements were recorded between 60 and 160 °C for a water vapor pressure of 10 kPa. Preliminary tests demonstrated that extremely long equilibration times (more than a week) were needed below 60 °C. At the end of each temperature equilibration, water content and density (ρ) of the acid solution of the cell were determined. For these purposes, a small aliquot of acid solution was transferred into a preheated 5 ml glass bottle also stored in the climate chamber and tightly sealed with a minimum of gas volume using a polytetrafluoroethylene-protected silicon septum. After rapid cooling to 23 °C, the acid solution was transferred to a *Metrohm 852 Titrando* using a syringe through the septum. The water content (m) of each acid solution was determined using the Karl-Fischer titration methods and Hydranal standard solutions. For acid solutions with water contents below 3 wt%, the coulometric titration method was used; otherwise the volumetric determination was selected. The titration was repeated five times for each extract of acid solution. The solution density was determined before and after each titration considering weight and volume of the syringe.

3. RESULTS AND DISCUSSION

3.1. Density and Water Content

The water content, in terms of water concentration (m) in the aqueous solutions of H_3PO_4, and density (ρ) were determined independently via titration and weighting after the establishment of a thermodynamic equilibrium for a certain temperature, as specified in the experimental section. As shown in Fig. 2, the two parameters have a strong correlation. In order to adequately represent the large water content, data are presented in the figure in logarithmic scale. The experimental data show a good agreement with the results provided by MacDonald *et al*. [19], [20] for H_3PO_4 in the concentration range 86–102 wt%, from room temperature to 170 °C.

It is known that, by increasing temperature, H_3PO_4 forms pyrophosphoric acid ($H_4P_2O_7$) and water in a condensation reaction:

$$2\ H_3PO_4 \rightleftarrows H_4P_2O_7 + H_2O \tag{1}$$

By decreasing water activity/partial pressure, in subsequent condensation steps, triphosphoric acid ($H_5P_3O_{10}$) is formed

$$H_4P_2O_7 + H_3PO_4 \rightleftarrows H_5P_3O_{10} + H_2O, \tag{2}$$

while higher oligomers, like $H_6P_4O_{13}$ and $H_7P_5O_{15}$, are formed successively. The formation of different coexisting phosphoric acid condensates, with an increasing polymerization degree depending on temperature and water partial pressure, ultimately leads to a system with complex kinetic processes. Therefore, for certain temperature ranges and water contents, different mixtures of condensates can exist either in a stable or metastable state [21], [22].

Fig. 2 shows three different behaviours of the dependency of H_3PO_4 density from H_2O content of the acid solutions. The behaviours are characterized by three different slopes of the interpolating linear function so that three regions can be marked in Fig. 2. In the first region (I), the water content is high (from 100 to 12 wt% H_2O) and no H_3PO_4 condensates are expected. The density is low but increases very fast due to a decreasing water content until a maximum of 1.7 g·cm^{-3}. The second and intermediate region (II) between 6–12 wt% H_2O is characterized by a steady increase of the fraction of condensates, like pyrophosphoric and triphosphoric acid, as indicated in Eq. (1), Eq. (2) [23]. Finally, the third region (III) is

characterized by phosphoric acid solutions with very low water content, where the density values do not change significantly around the value of 1.8 g·cm^{-3}.

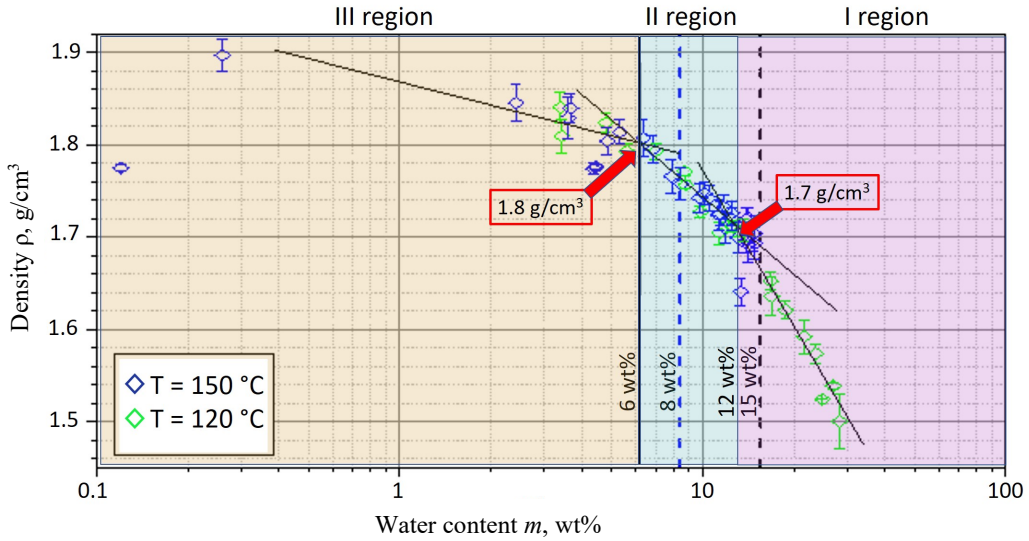

Fig. 2. Correlation between density ρ and water content *m* of the phosphoric acid solutions at 120 °C (green) and 150 °C (blue). Vertical lines mark particular compositions discussed in the text. Three regions are highlighted.

It is worth to note that the density of neat H_3PO_4 at 25 °C is 1.87 g·cm^{-3}, so that in this region the composition is almost neat ortho-phosphoric acid. No evidences of composition changes are observable: The condensate formation/dissolution and structural effects are less dominant and rehydration process occurs. The results can be used to model the vapor-liquid equilibrium of water and the concentration of phosphoric acid in the PEMFCs [24].

3.2. Thermal Equilibrium

One of the phenomena studied in this work is the thermodynamic equilibrium, and its relaxation kinetics, between the liquid H_3PO_4 solution and the surrounding water vapor when the relative humidity is changed, *i.e.* the water activity (partial pressure). Phosphoric acid solutions are characterized by high heat of solution so that a small change in water content induces a significant temperature change, as reported also by Luff *et al.* [25] and Jones *et al.* [26].

The design of the experimental setup used for the present investigation was optimized in a way that the mass (water) exchange at the surface is limiting. Indeed, the liquid surface area in the quartz cell is relatively small (157 cm^2) compared to the total volume of the solution (500 cm^3), as well the bulk of the liquid is vigorously mixed by the see-saw mechanism. The kinetics of the water concentration change in the phosphoric acid solution can be described by an exponential decay function and the half-time parameter τ can be obtained, see Fig. 3. This approach provides good fits with a high confidence level while introducing a minimum number of variables. The other parameters, such as the pre-exponential factor or the offset, depend on the previous state of the solution and no meaningful correlation was found. Another limitation is the minimum time needed for the climate chamber to adjust to new conditions. Nevertheless, this time was found to be in the range of 10^3 s, *i.e.* ca. 17 min.

Therefore, the lower limit for the thermal half-time was set to this value in order to avoid interference between the system response and the water-uptake/loss kinetics of the phosphoric acid. As presented in Fig. 3, all experimental data have values of τ significantly greater than 10^3 s, *i.e.* between 2 hours and 1 day of equilibration time.

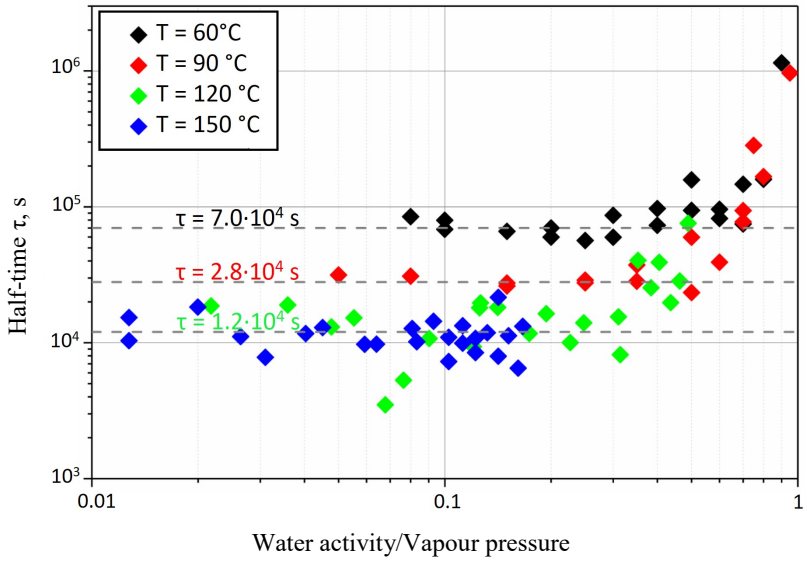

Fig. 3. Half-time *τ* of the water exchange kinetics of the phosphoric acid solutions as function of the water activity/vapour pressure in the gas phase.

The assumption of a surface-limited water exchange kinetics in the setup is no longer valid for the 150 °C dataset. A transition to a volume diffusion-limited kinetics occurred. Studies in this direction are in progress. However, the time evolution of the electrical impedance data was still following an exponential decay function.

Another interesting feature is that for each temperature, a certain water vapor activity threshold exists. Below this activity, the half-time parameter *τ* remains almost constant. However, an unambiguous correlation with a specific water content could not be established yet. As expected, the τ values increase significantly with decreasing temperature. Surprisingly, the τ values increase with increasing water activity, *i.e.* with increasing water content. This suggests a slow kinetics of the equilibration process in the case of a high dilution of the phosphoric acid solution [27].

By applying an Arrhenius-type equation [28] to the limiting asymptotes for decreasing water activity, using the values for τ (60 °C) of ~$7 \cdot 10^4$ s, τ (90 °C) of ~$2.8 \cdot 10^4$ s and τ (120 °C) of ~$1.2 \cdot 10^4$ s, a thermal activation energy of about 14 kJ·mol^{-1} is obtained. This value is related to the water exchange kinetics between liquid and gas phase und thus agrees with the enthalpy of dilution (of a phosphoric acid solution with a certain composition). In the case of 85 wt% H_3PO_4 at 25 °C, the enthalpy of dilution has a value of 13.5 kJ mol^{-1}, as determined by Jones *et al.* [26]. The enthalpy of evaporation of water has a value of approximately 43 kJ·mol^{-1}, as given by MacDonald *et al.* [19] More detailed data is summarized by Korte [6]. Thus, this ascertains the assumption that the temperature dependence of water exchange kinetics is rather limited by the dilution than the evaporation process.

The good agreement with the literature data also validates the reliability of the used setup and the methodologic approach to study the vapor-liquid equilibrium [23]. This is particularly necessary to understand dynamic operations in a HT-PEMFC, where a change of the electric load and thus of the cathodic water production/stationary water vapor pressure will cause a redistribution of the phosphoric acid in the membrane [29], [30].

3.3. Electrical Conductivity

The conductivity of the phosphoric acid solutions depends strongly on the water content and thus also on the water vapor partial pressure. However, additional processes like the dimerization and further condensation processes take place in the acid solution, which may also influence the proton transport [31]. These processes are extremely critical for the performances of the PEMFCs, which strongly depend on the amount of H_3PO_4 in the polymer membranes [32]. In the present study, the electrical impedance was directly measured at the thermal equilibrium by the Iviumstat electrochemical interface. Successively, the impedance values were converted into the electrical conductivity κ.

In Fig. 4 the conductivity of H_3PO_4 solutions in thermodynamic equilibrium at four different temperatures is plotted as a function of the water activity/vapor partial pressure. As expected, κ increases with increasing water content. For the 60 °C and 90 °C dataset a strong drop of the conductivity is observable after the maximum value of κ is reached.

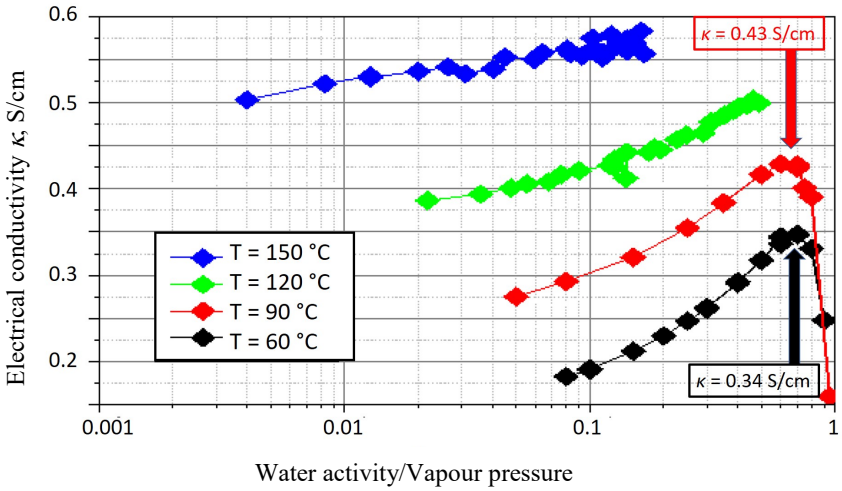

Fig. 4. Electrical conductivity κ of phosphoric acid solutions *vs*. water activity/vapour partial pressures at four different temperatures: 150 °C (blue), 120 °C (green), 90 °C (red), and 60 °C (black).

The maxima of κ can be observed at a water content higher than 30 wt%, which is in good agreement with the results of Melchior *et al*. [11] and the compilation of Korte [6]. In the case of the higher temperatures, i.e. at 120 °C and 150 °C, the performances of the climate chamber were insufficient to reach the requested high water vapor pressure to detect the expected maxima.

In Fig. 5 the conductivity data is depicted by using a colour gradient. The κ values are plotted as a function of the water activity/vapor partial pressure and the reciprocal temperature $1/T$. Additionally, a polynomial fit function is inserted in Fig. 5 as overlay lines. The maximum of the conductivity shifts with increasing water activity to lower temperatures.

For temperatures above 120 °C the maximum of κ for the phosphoric acid solutions cannot be reached using atmospheric pressure conditions: The cross-barred area in Fig. 5 is not accessible, as the water vapor pressure would exceed the atmospheric pressure.

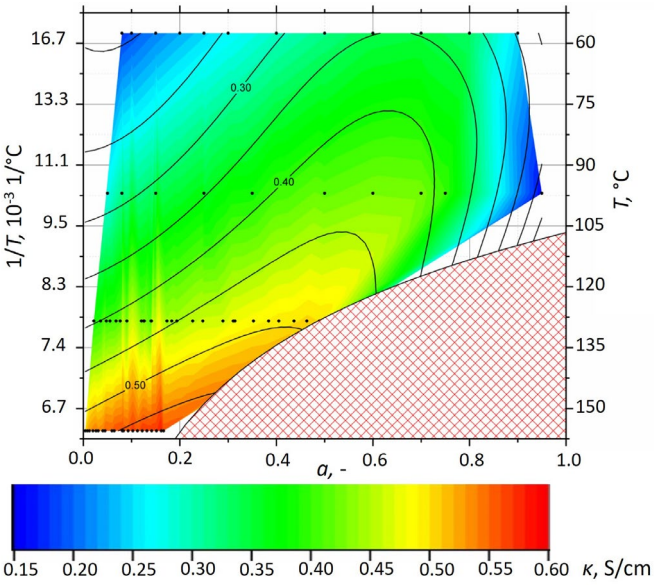

Fig. 5. 3D representation of the temperature and water activity dependence of the electrical conductivity κ (colour coded) of phosphoric acid solutions. See text for explanation of the cross-barred area.

4. CONCLUSION

In this work, a new setup for conductivity measurements at controlled water vapor partial pressure, temperature and exchange area to the gas phase is presented and tested. An extensive dataset of experimental electrical conductivity data for phosphoric acid solutions at different water activities is measured. The results are compared to literature data to validate the reliability of the developed setup and the methodologic approach. Data were acquired from 60 to 150 °C, *i.e.* in a temperature range which is also relevant for phosphoric acid-based polymer electrolyte membrane fuel cells. The influence of the water activity/vapor partial pressure and temperature is provided in relation with the density and electrical conductivity.

In general, the results are in good agreement with the data found in the literature. Two clustering points at density values of 1.7 g·cm^{-3} and 1.8 g·cm^{-3} are observed, although the water content is changing. This indicates transitions within the phosphoric acid solutions like the formation of phosphoric acid condensates or rehydration processes between orthophosphoric acid and pyrophosphoric acid.

The condensation/rehydration process of phosphoric acid solutions was discussed in terms of density *vs.* weight fraction of water. The experimental data were fitted using linear interpolation and two transitions were detected in correspondence of three different steepness of the linear functions. The first transition was attributed to the ortho-/pyro-phosphoric acid transition at low water contents, *e.g.* below 8 wt%. The second transition, at about 12 wt% water content, was attributed to a dilution effect which disaggregates the H_3PO_4 condensates.

The developed setup in quartz allows the measurements of the electrical conductivity of the phosphoric acid solutions. An increment was observed by increasing the temperature: At 60 °C the maximum conductivity was recorded at 0.34 S/cm while at 90 °C the maximum was observed at 0.43 S/cm.

The water exchange rate was found to be almost independent to the water activity/vapor partial pressure for water contents below 15 wt% and is strongly decreasing for higher water contents. These water contents represent concentrated H_3PO_4, *i.e.* about 85 wt%. The water exchange rate was found to be thermally activated and, for the temperature range between 60 and 120 °C, an activation energy of about 14 kJ·mol^{-1} was estimated. This is close to the value of the enthalpy of dilution.

The performances of HT-PEMFCs are strongly related to the amount of H_3PO_4 in the polymer membrane. Indeed, the proton conductivity of the membrane depends on the equilibria in the H_2O-H_3PO_4 system, i.e. hydrolysis, protolysis and condensation equilibria. The present results gain more insights into the exceptional conductivity of phosphoric acid, whose mechanism remains a very complex puzzle. Additionally, the experimental values can be used as starting data set to model the vapor-liquid equilibrium of water in phosphoric acid solutions.

Finally, the agreement between the literature data and the experimental results obtained with the developed setup suggests the possibility of further studies of the vapor-liquid equilibrium in in the H_2O-H_3PO_4 system. These studies are particularly necessary to understand dynamic operations in HT-PEMFCs, where a change of the electric load and thus of the cathodic water production/stationary water vapor pressure will cause a redistribution of the phosphoric acid in the membrane and consequently a change in the performances.

ACKNOWLEDGEMENT

This work has been supported by the European Union's Horizon 2020 EIT Raw Materials research and innovation program under the grant agreement n. 19247, project 'ALPE'. The authors would like to thank Mrs. Katja Klafki for helpful cooperation.

REFERENCES

[1] Zhao J., Li X. A review of polymer electrolyte membrane fuel cell durability for vehicular applications: Degradation modes and experimental techniques. *Energy Conversion and Management* 2019:199:112022. https://doi.org/10.1016/j.enconman.2019.112022

[2] Zhang J., *et al*. Advancement toward polymer electrolyte membrane fuel cells at elevated temperatures. *Research* 2020:9089405. https://doi.org/10.34133/2020/9089405

[3] Tabassum N., Islam N., Ahmed S. Progress in microbial fuel cells for sustainable management of industrial effluents. *Process Biochemistry* 2021:106:20–41. https://doi.org/10.1016/j.procbio.2021.03.032

[4] Marks J., *et al*. Effect of combining different substrates and inoculum sources on bioelectricity generation and COD removal in a two-chambered microbial fuel cell: A preliminary investigation. *Environmental and Climate Technology* 2020:24(2):67–78. https://doi.org/10.2478/rtuect-2020-0055

[5] Pahari S., Roy S. Structural and conformational properties of polybenzimidazoles in melt and phosphoric acid solution: A polyelectrolyte membrane for fuel cells. *RSC Advances* 2016:6:8211–8221. https://doi.org/10.1039/c5ra22159e

[6] Korte C. Phosphoric Acid, an Electrolyte for Fuel Cells – Temperature and Composition Dependence of Vapor Pressure and Proton Conductivity. In *Fuel Cell Science and Engineering*. Wiley, 2012, pp. 335–359.

[7] Korte C., *et al*. Phosphoric Acid and its Interactions with Polybenzimidazole-Type Polymers. In Li Q., Aili D., Hjuler H., Jensen J. (eds) *High Temperature Polymer Electrolyte Membrane Fuel Cells*. Springer, 2016, pp. 169–194. https://doi.org/10.1007/978-3-319-17082-4_8

[8] Rodier M., *et al*. Determination of Water Vapor Pressure over Corrosive Chemicals Versus Temperature Using Raman Spectroscopy as Exemplified with 85.5% Phosphoric Acid. *Applied Spectroscopy* 2016:70:1186–1194. https://doi.org/10.1177/0003702816652362

[9] Halter J., *et al*. Breaking through the Cracks: On the Mechanism of Phosphoric Acid Migration in High Temperature Polymer Electrolyte Fuel Cells. *Journal of Electrochemical Society* 2018:165(14):F1176–F1183. https://doi.org/10.1149/2.0501814jes

[10] Di Noto V., *et al*. Effect of high pressure CO_2 on the structure of PMMA: A FT-IR study. *Journal of Physical Chemistry B* 2011:115:13519–13525. https://doi.org/10.1021/jp207917n

[11] Melchior J.-P., Kreuer K.-D., Maier J. Proton conduction mechanisms in the phosphoric acid-water system (H4P2O7-$H_3PO_4 \cdot 2H_2O$): A ^{1}H, ^{31}P and ^{17}O PFG-NMR and conductivity study. *Physical Chemistry Chemical Physics* 2017:19:587–600. https://doi.org/10.1039/C6CP04855B

[12] Vilčiauskas L., *et al*. The mechanism of proton conduction in phosphoric acid. *Nature Chemistry* 2012:4:461–466. https://doi.org/10.1038/nchem.1329

[13] Heres M., *et al*. Proton Conductivity in Phosphoric Acid: The Role of Quantum Effects. *Physical Review Letters* 2016:117:156001. https://doi.org/10.1103/PhysRevLett.117.156001

[14] Bakher Z., Kaddami M. Thermodynamic equilibrium study of phosphorus pentoxide-water binary system: The stability and solubility of $10H_3PO_4 \cdot H_2O$. *Calphad* 2018:63:148–155. https://doi.org/10.1016/j.calphad.2018.09.006

[15] Aili D., *et al*. Phosphoric acid dynamics in high temperature polymer electrolyte membranes. *Journal of The Electrochemical Society* 2020:167:134507. https://doi.org/10.1149/1945-7111/abb70c

[16] Mifsud C., Fujioka T., Fink D. Extraction and purification of quartz in rock using hot phosphoric acid for in situ cosmogenic exposure dating. *Nuclear Instruments and Methods in Physics Research Section B: Beam Interactions with Materials and Atoms* 2013:294:203–207. https://doi.org/10.1016/j.nimb.2012.08.037

[17] Shreiner R. H., Pratt K. W. Primary Standards and Standard Reference Materials for Electrolytic Conductivity. Gaithersburg: NIST, 2004.

[18] McKee C. B. An accurate equation for the electrolytic conductivity of potassium chloride solutions. *Journal of Solution Chemistry* 2009:38:1155–1172. https://doi.org/10.1007/s10953-009-9436-x

[19] MacDonald D. I., Boyack J. R., Density, electrical conductivity, and vapor pressure of concentrated phosphoric acid. *Journal of Chemical & Engineering Data* 1969:14380–384. https://doi.org/10.1021/je60042a013

[20] Jiang X., *et al*. Density, viscosity, and thermal conductivity of electronic grade phosphoric acid. *Journal of Chemical & Engineering Data* 2011:56(2):205–211. https://doi.org/10.1021/je100938j

[21] Majerus A., *et al*. Thermogravimetric and spectroscopic investigation of the interaction between polybenzimidazole and phosphoric acid. *ECS Transactions* 2013:50(2):1155–1165. https://doi.org/10.1149/05002.1155ecst

[22] Conti F., *et al*. Carbon NMR investigation of the polybenzimidazole-dimethylacetamide interactions in membranes for fuel cells. *New Journal of Chemistry* 2013:37:152–156. https://doi.org/10.1039/c2nj40728k

[23] Lang S., *et al*. Diffusion coefficients and VLE data of aqueous phosphoric acid. *Journal of Chemical Thermodynamics* 2014:68:75–81. https://doi.org/10.1016/j.jct.2013.08.028

[24] Kazdal T.J., *et al*. Modelling of the vapour-liquid equilibrium of water and the in situ concentration of H3PO4 in a high temperature proton exchange membrane fuel cell. *Journal of Power Sources* 2014:249:446–456. https://doi.org/10.1016/j.jpowsour.2013.10.098

[25] Luff B. B. Heat capacity and enthalpy of phosphoric acid. *Journal of Chemical & Engineering Data* 1981:26:70–74. https://doi.org/10.1021/je00023a023

[26] Jones G. P., Lee D. A. The enthalpy of dilution of concentrated orthophosphoric acid. *Journal of Chemical Thermodynamics* 1970:2:760–761. https://doi.org/10.1016/0021-9614(70)90053-4

[27] Fleige M., *et al*. Evaluation of temperature and electrolyte concentration dependent Oxygen solubility and diffusivity in phosphoric acid. *Electrochimica Acta* 2016:209:399–406. https://doi.org/10.1016/j.electacta.2016.05.048

[28] Petrowsky M., Frech R. Temperature dependence of ion transport: The compensated Arrhenius equation. *Journal of Physical Chemistry B* 2009:113:5996–6000. https://doi.org/10.1021/jp810095g

[29] Eberhardt S. H., *et al*. Dynamic operation of HT-PEFC: In-operando imaging of phosphoric acid profiles and (re)distribution. *Journal of The Electrochemical Society* 2015:162:F310–F316. https://doi.org/10.1149/2.0751503jes

[30] Boillat P., *et al*. Evaluation of neutron imaging for measuring phosphoric acid distribution in high temperature PEFCs. *Journal of The Electrochemical Society* 2014:161:F192–F198. https://doi.org/10.1149/2.023403jes

[31] Conti F., *et al*. Phase diagram approach to study acid and water uptake of polybenzimidazole-type membranes for fuel cells. *ECS Transactions* 2016:72:157–167. https://doi.org/10.1149/07208.0157ecst

[32] Korte C., *et al*. Uptake of protic electrolytes by polybenzimidazole-type polymers: absorption isotherms and electrolyte/polymer interactions. *Journal of Applied Electrochemistry* 2015:45:857–871. https://doi.org/10.1007/s10800-015-0855-7